Mechanical behavior and magnetic separation of quasi-one-dimensional SnO_2 nanostructures: A technique for achieving monosize nanobelts/nanowires

Z. Q. Jin
School of Materials Science and Engineering, Georgia Institute of Technology, Atlanta, Georgia 30332 and Department of Physics, University of Texas at Arlington, Arlington, Texas 76019

Y. Ding
School of Materials Science and Engineering, Georgia Institute of Technology, Atlanta, Georgia 30332

Z. L. Wang[a)]
School of Materials Science and Engineering, Georgia Institute of Technology, Atlanta, Georgia 30332 and National Center for Nanoscience and Nanotechnology, and International Quantum Structure Center, Institute of Physics, CAS, Beijing, 100080, China

(Received 10 November 2004; accepted 3 February 2005; published online 25 March 2005)

The as-synthesized nanowires and nanobelts usually have a large size distribution. We demonstrate here a ball milling technique for narrowing the size distribution of oxide nanobelts and nanowires. High-resolution scanning and transmission electron microscopy reveals that the one-dimensional SnO_2 nanostructures with size >150 nm are sensitive to the milling effect and most of them were fractured into nanoparticles even after a short-time milling. These nanoparticles contain magnetic Fe components, which could be effectively separated from those nanobelts by employing a magnetic field. This feature promises a potentials application in the nanostructured materials separation. It was also found that the dominant size of the survived nanostructures is <100 nm. The good mechanical behavior of the nanostructures are not only related to the superior mechanical toughness due to small size, but also related to the low defect density. © *2005 American Institute of Physics*. [DOI: 10.1063/1.1882774]

I. INTRODUCTION

Nanostructured materials are the foundation of nanotechnology.[1–9] Due to their unique morphology and small sizes, nanomaterials exhibit unique, largely improved properties compared to the coarse-grained bulk materials. Among these nanostructures, functional oxides have drawn much attention since they can be used for fabricating nanodevices.[10] Quasi-one-dimensional (Q1D) structured tin oxides have, for example, potential applications in optoelectronic devices, gas sensors, and field-effect transistors.[11–13] The SnO_2 nanobelts may also be very suitable as cantilevers for atomic force microscopy due to their unique morphology, semiconducting characteristic and much reduced sizes.[14] Upon being considered for such applications, the mechanical behavior of these materials is an important factor, especially with the increased surface-to-volume ratio. One of the critical issues in grasping the unique mechanical properties of Q1D oxides is to understand their size effect. For instance, most recent studies[15] revealed that the elastic modulus of lead and silver nanowires and polypyrrole nanotubes with diameter smaller than 30 nm drastically increases.

In general, there exist various Q1D nanostructures, including nanowires, nanoribbons, nanotubes, and nanobelts, in the products prepared using thermal evaporation.[1] The nanostructures, with diversity in size, growth direction and morphology, coexist in the as-synthesized sample. Techniques have been developed for measuring the effective bending modulus of individual nanowire/nanobelt.[16–19] Recently, it was reported that mechano-thermal method consisting of mechanical milling and subsequent thermal annealing was able to prepare Q1D nanostructures.[20–23] The ball milling method has also been successfully utilized to cut carbon nanotubes from long nanotubes by collision between milling ball and nanostructured powders.[24,25] It thus suggests that low-energy mechanical ball milling technique might be an effective method for evaluating the overall mechanical properties of different nanostructures under collision among steel balls. During the milling process, the impurities originated from the milling jar and steel ball will inevitably result in a nonuniform structure and may affect the properties of nanostructures. These Fe-containing impurities exhibit magnetic behavior and might be easily removed by employing a magnetic field onto the milled materials, the so-called magnetic separation technique. This technique takes advantage of the different responses of these nanostructured components to the magnetic field. Recently, the magnetic separation has also been commercially used for drug delivery, selection of biomolecules, and DNA separation and purification. In these applications, the introduction of magnetic component into the nanostructure was generally carried out by the dopping approach or using superparamagnetic core particle. These nanostructures are thus allow themselves to be separated

[a)]Author to whom correspondence should be addressed. Electronic mail: zhong.wang@mse.gatech.edu

from other solution or mixed matrix using a permanent magnet or electromagnet and easily selected for specific application.

In this paper, the mechanical behavior of SnO_2 nanobelts before and after low-energy ball milling was compared. Since magnetic components were introduced during the milling process, subsequent magnetic separation was employed. A different milling effect on the fracture of the nanobelts with different sizes was observed. It reveals that the one-dimensional nanostructures with size >150 nm are sensitive to the milling effect and most of them were broken even after a short-time milling, accompanied with the introduction of soft magnetic component Fe into the nanoparticles. These nanoparticles can be separated by the magnetic separation technique. The dominant size of the survived nanowires/nanobelts is <100 nm. This work demonstrates a technique for unifying the size of the as-synthesized nanobelts and nanowires.

II. EXPERIMENTAL PROCEDURE

SnO_2 nanobelts were synthesized by thermal evaporation of oxide powders at high temperature by controlling the gas flow rate, annealing temperature, and evaporation time. The detailed synthesis process has been reported previously.[2] Thermal evaporation of SnO/SnO_2 powders was performed at 1050–1150 °C. At elevated temperatures, the products were deposited onto several alumina plates. The as-received growth product was milled for 6 h at room temperature in a Spex 8000 mixer. The milling system contains several 3 -mm-diameter stainless-steel balls, and the mixture ratio of the steel balls and growth product was selected to be $\sim 50:1$ in weight percent. Hexane was used as surfactant to get much uniform milling effect. Subsequent magnetic separation was preliminarily employed using a commercial magnet while the nanomaterial was ultrasonically vibrated in the hexane medium so as to achieve a better separation effect.

The as-deposited and milled samples were then characterized by scanning electron microscopy (SEM) (LEO 1530 FEG), and transmission electron microscopy (TEM) [Hitachi HF-2000 FEG with energy-dispersive x-ray spectroscopy (EDS) at 200 kV and a JEOL 4000 EX high-resolution TEM (HRTEM) at 400 kV].

III. RESULTS AND DISCUSSION

After evaporation and deposition, a large amount of long nanobelts was observed except for some nanosized particles. Figures 1(a) and 1(b) are typical SEM images displaying the morphologies of the nanobelts before and after ball milling, respectively. EDS analysis and electron diffraction show that the nanobelts are SnO_2. The as-synthesized SnO_2 nanobelts have a large size distribution with the width w varying from several tens of nanometers to several hundred nanometers and lengths of dozens of micrometers. All the nanobelts with $w>150$ nm are straight. The irregular surface configuration apparently originates from the imperfect grain growth during the deposition process. It is noticed that nanobelts with $w<100$ nm have curly morphology, demonstrating the high mechanical flexibility.

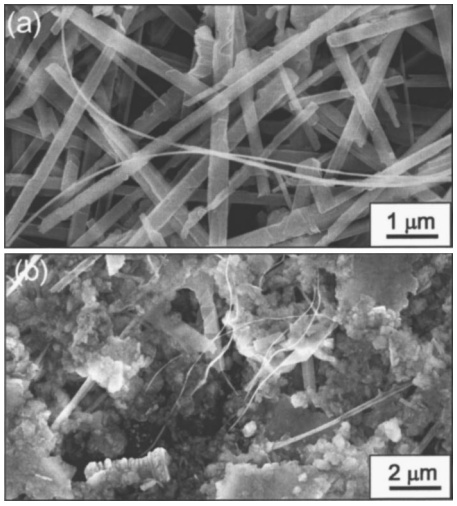

FIG. 1. SEM images of the SnO_2 nanobelts before (a) and after (b) ball milling process.

After ball milling, most of the large size nanobelts have been fractured into small particles, but the small size nanobelts survived. This is the most striking feature of the mechanical alloying process. The thin nanobelts can be bent or twisted easily to various degrees without rupture, while those unbending large nanobelts either fracture or have been ground into agglomerated nanoparticles. No contamination of Fe from milling vessel and/or balls was detected in the milled nanobelts, while the nanoparticles contain a significant amount of Fe as revealed by EDS patterns.

The plots in Fig. 2 give the detailed size distributions of the nanobelt width before and after ball milling. The dominant size distribution of the original nanobelts is wide in a range from 50 to 300 nm, however a much narrow size distribution with peak between 50 and 100 nm is evident after ball milling. The milling process effectively narrows the size distribution of the nanobelts and preserves the small size nanobelts. The grinding and collision of balls result in the fracture of large-size nanobelts and the increase of volume fraction of nanoparticles.

In order to separate those nanoparticles embedded with magnetic iron from the nanobelts, a permanent magnet was

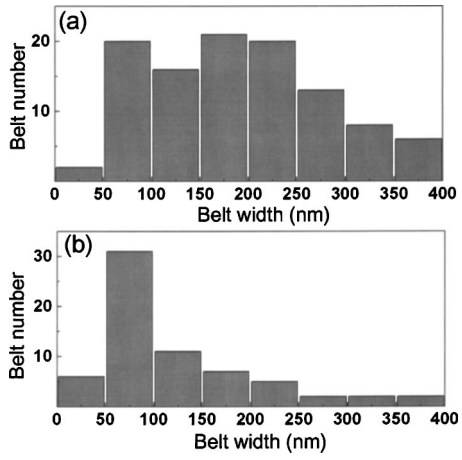

FIG. 2. Plots of the nanobelt size distributions before (a) and after (b) ball milling process.

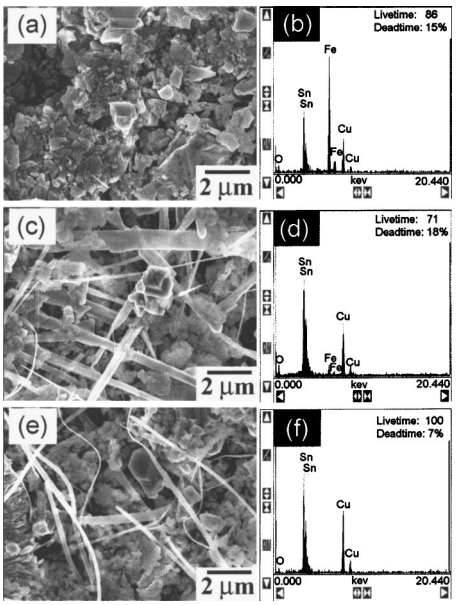

FIG. 3. SEM images and EDS patterns of the milled samples subjected to the magnetic separation. (a) Magnetic attracted particles. (c) Nanobelts with magnetic particles attached on the surface. (e) Nanobelts not subjected to the magnetic attractive force. (b), (d), (f) are the correlated EDS patterns to (a) particles, (c) large-size nanobelts, and (e) small-size nanobelts.

used for the magnetic separation. The separation principle was based on the balance among the magnetic force, buoyant force and gravitational force, as described by

$$F(B) = \frac{\chi}{\mu_0} B \frac{dB}{dz} + \rho_l g - \rho_n g,$$

where χ is the magnetic susceptibility of milled materials, μ_0 is the vacuum permeability, B is the magnetic field strength, z depicts the field direction, g is the gravity acceleration, ρ_l *and* ρ_n are the density of liquid and nanomaterials, respectively. When $F(B) > 0$, the materials will be attracted to the magnet pole, and consequently, the materials will move downward due to the gravity, thus leading to the materials separation. Because ρ_l *and* ρ_n almost remain same in our case, one may assume that the force $F(B)$ is predominately associated with the spatial distribution of magnetic field and the measurement of volume susceptibility χ. The χ value is closely associated with the content of impurity Fe in the nanomaterials since tin oxide has an extremely low susceptibility compared with Fe. It is reasonable that the materials with high component of Fe will be more subjected to the external magnetic field. Figure 3 shows the SEM images and EDS patterns of milled samples subjected to a magnetic field (around 0.3–0.5 T). Apparently, the nanomaterials with different morphology differ in how they interact with a magnetic field. The particles are very sensitive to the external field as shown in Fig. 3(a), verifying that soft magnetic Fe has embedded in these agglomerates due to the mechanical milling, which is consistent with the composition analysis by EDS [Fig. 3(b)]. The large-size nanobelts surrounded by the agglomerated particles are also subjected to the attraction of magnetic field as shown in Fig. 3(c), while the fraction of Fe on the nanobelts as shown in Fig. 3(d) is apparently lower than those of particles. The Fe mostly attaches on the surface

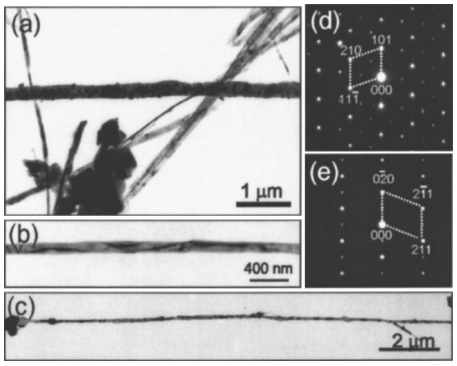

FIG. 4. Typical SnO_2 belts of different sizes before ball milling. The SAED patterns in (d) and (e) coming from the large belts in (a) and thin belt in (b), respectively. The superlattices in (d) indicate the existence of orthorhombic structured SnO_2.

of nanobelts. It is evident from Fig. 3(e) that those unstrained nanobelts of small size are free from Fe contamination as revealed in Fig. 3(f) and not subjected to the attraction of magnetic field, verifying the better anticontamination ability for these small nanobelts during the milling process. However it is reasonable that the magnetic separation still suffers from one difficulty. It is impossible to completely eliminate magnetic impurities due to the existing agglomeration under milling. However, this approach has the potential in the separation of nanomaterials according to their inherent characteristic under an optimal combination condition of milling and magnetic separation technique.

In order to characterize the structures of the nanobelts before and after ball milling, TEM images and selected-area electron diffraction (SAED) patterns were recorded from the samples. Low magnification TEM images recorded from large and small belts before ball milling are displayed in Fig. 4. The SAED patterns of the large belt in Fig. 4(a) and the thin belt in Fig. 4(b) are displayed in Figs. 4(d) and 4(e), respectively. The basic diffraction spots for the large-scale nanobelts can be indexed using the SnO_2 tetragonal structure. The extra weak diffraction spots in Fig. 4(d) are from the SnO_2 orthorhombic structure, which has been discussed in detail in Ref. 2. The large nanobelts are composed of orthorhombic and tetragonal phases distributed as domains. Combining the images and the SAED patterns, the main growth front planes of the nanobelts are $(201)_{\text{Tetragonal}}$ and $(110)_{\text{orthorhombic}}$, which are the same as those in Ref. 2. The structural hybrid nanobelts are the dominant products before ball milling. However, the superlattice structure does not exist in the thin nanobelts which show a much more uniform and perfect tetragonal structure with $(201)_{\text{tetragonal}}$ as the growth plane front [Fig. 4(e)]. These single crystalline thin nanobelts can be dozens of micrometers in length. The contrast observed is due to the bending contour.

After ball milling, two typical nanobelts with width of 80 and 50 nm are shown in Fig. 5(a). The inset SAED pattern from the large nanobelt indicates that the nanobelt retains its single crystalline tetragonal structure with the growth front plane of $(201)_{\text{tetragonal}}$, which is the same as that of the belt in Fig. 4(b). Its uniform contrast indicates that the belt is dislocation free. It is noticed that the thickness of the

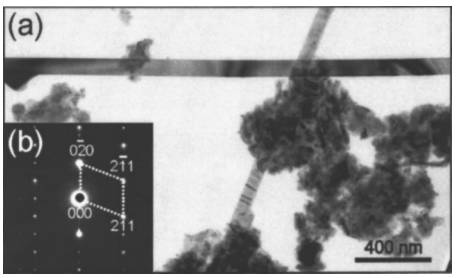

FIG. 5. (a) Nanobelt survived after the ball milling process. The SAED pattern (inset) shows the growth front plane is (201). Its uniform contrast in the enlarged image (b) indicates it is dislocation-free.

thin nanobelts is still quite uniform even after ball milling. A phenomenon that should be emphasized is that the percentage of the orthorhombic structured nanobelts decreases after ball milling. In general, the existence of the orthorhombic phase usually results in wide nanobelts due to the coexistence of the orthorhombic and tetragonal phases. The wider nanobelts are easier to be fractured, thus, they vanished from the belt shape after ball milling, demonstrating that ball milling is useful in purifying the phase of the nanobelts.

Besides the nanobelts described above, we also found many belts taking the $(2\bar{2}1)$ plane as their growth front before and after the ball milling process. Figure 6(a) shows a nanobelt that survived ball milling. The inset is an enlarged image of the belt. The contrast in the image is attributed to the strain induced bending effect. Figures 6(b) and 6(c) are the SAED pattern and HRTEM image of the belt in Fig. 6(a). The HRTEM image of the nanobelt displays a dislocation-free volume in the milled samples. Although several types of nanobelts were observed in our experiments, it seems that the mechanical behavior of the SnO_2 nanobelts is sensitive to their size rather than their growth directions.

Our results are different from the previous report[24] on the ball milled carbon nanotubes, in which the small nanotubes cleave much faster than large tubes and no other forms of carbon except nanotubes were observed even after long time of milling. It is believed that, with the increase of ball milling time, more and more particles and their agglomerates form (Fig. 1). The large-scale rigid nanobelts fracture not only at the impact sites but also at the structural defect sites (such as dislocations and domain boundaries). The flexible thin nanobelts can be curved freely in three dimensions without fracture.

Since collision and friction between balls and nanobelts play a dominant role on the bending or fracture of nanotubes, there may exist other possibilities for the size-related milling effect. For instance, for large-scale rigid nanobelts with more impacting surface, the ball's collision could be more effective; while for one-dimensional nanomaterials with reduced size, the elastic modulus could be higher than those of large diameters.[15] Therefore, narrow nanobelts survive from ball collision more preferentially than large nanobelts due to better mechanical behavior.

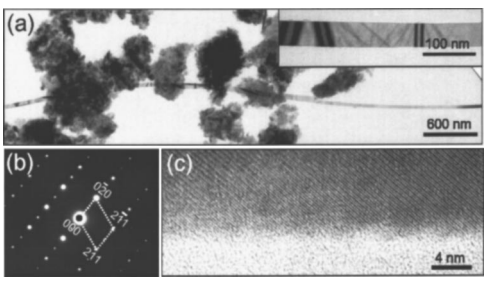

FIG. 6. Low magnification (a) and enlarged (inset) TEM images and the corresponding SAED pattern (b) from a nanobelt after ball milling, showing the growth front plane of $(2\bar{2}1)$, (c) is a HRTEM image of the belt.

IV. CONCLUSIONS

The mechanical response of SnO_2 nanobelts with different width was investigated using low-energy ball milling process. It is found that the flexibility of one-dimensional nanostructured tin oxides increases with decreasing size. The one-dimensional nanostructures with size >150 nm are sensitive to ball milling and most of them were broken, accompanied with the increase in the volume fraction of nanoparticles even after short-time milling. These nanoparticles can be effectively separated from the nanobelts by magnetic separation technology. Although the larger the magnetic field is, the stronger is the magnetic attractive force. It is unnecessary to use very high magnetic field since the separation capability depends more on the difference in susceptibility of different materials. When this technique was adopted in conjunction with milling technology for the nanomaterials with different mechanical properties, it should be more effective in the separation. It has been shown that thin nanobelts with $w<100$ nm apparently have much better mechanical response to ball milling. The good mechanical properties of the nanostructures are not only related to the small size (<100 nm), but also to low dislocation density. The mechanical ball milling is likely an effective method for separating small-scale structure from the large-scale Q1D structure. This could be very useful for future applications.

ACKNOWLEDGMENT

The authors acknowledge generous support by the Defense Advanced Projects Research Agency, NASA, National Science Foundation, CAS of China.

[1] Z. W. Pan, Z. R. Dai, and Z. L. Wang, Science **209**, 1947 (2001).
[2] Z. R. Dai, J. L. Gole, J. D. Stout, and Z. L. Wang, J. Phys. Chem. B **106**, 1274 (2002).
[3] D. N. Mcllroy, A. Alkhateeb, D. Zhang, D. E. Aston, A. C. Marcy, and M. G. Norton, J. Phys.: Condens. Matter **16**, R415 (2004).
[4] A. F. da Fonseca and D. S. Galvao, Phys. Rev. Lett. **92**, 175502 (2004).
[5] Y. Chen, M. J. Conway, and J. D. Fitzgerald, Appl. Phys. A: Mater. Sci. Process. **76**, 633 (2003).
[6] Y. Weizmann, F. Patolsky, I. Popov, and I. Winer, Nano Lett. **4**, 787 (2004).
[7] J. G. Wen, J. Y. Lao, D. Z. Wang, T. M. Kyaw, Y. L. Foo, and Z. F. Ren, Chem. Phys. Lett. **372**, 717 (2003).
[8] J. Kameoka, D. Czaplewski, H. Q. Liu, and H. G. Craighead, J. Mater. Chem. **14**, 1503 (2004).
[9] Y. Murata and M. Adachi, Chem. Lett. **33**, 488 (2004).
[10] Z. R. Dai, Z. W. Pan, and Z. L. Wang, Adv. Funct. Mater. **13**, 9 (2003).
[11] J. Q. Hu, X. L. Ma, N. G. Shang, Z. Y. Xie, N. B. Wong, C. S. Lee, and S. T. Lee, J. Phys. Chem. **106**, 3823 (2002).
[12] J. Watson, Sens. Actuators **5**, 29 (1984).
[13] M. S. Arnold, P. Avouris, Z. W. Pan, and Z. L. Wang, J. Phys. Chem. **107**, 659 (2003).
[14] W. Hughes and Z. L. Wang, Appl. Phys. Lett. **82**, 2886 (2003).

[15]S. Cuenot, C. Fretigny, S. Demoustier-Champagne, and B. Nysten, Phys. Rev. B **69**, 165410 (2004).
[16]E. W. Wong, P. E. Sheehan, and C. M. Lieber, Science **277**, 1971 (1997).
[17]P. Poncharal, Z. L. Wang, D. Ugarte, and W. A. De Heer, Science **283**, 1513 (1999).
[18]X. D. Bai, P. X. Gao, Z. L. Wang, and E. G. Wang, Appl. Phys. Lett. **82**, 4806 (2003).
[19]Z. L. Wang, Z. R. Dai, R. P. Gao, and J. L. Gole, J. Electron Microsc. **51**, S79 (2002).
[20]B. C. Kim, K. T. Sun, K. S. Park, K. J. Im, T. Noh, M. Y. Sung, S. Nahm, Y. N. Choi, S. S. Park, and S. Kim, Appl. Phys. Lett. **80**, 479 (2002).
[21]L. W. Yin, Y. Bando, M. S. Li, Y. X. Liu, andY. X. Qi, Adv. Mater. (Weinheim, Ger.) **15**, 1840 (2003).
[22]J. S. Lee, K. Park, M. I. Kang, I. W. Park, S. W. Kim, W. K. Cho, H. S. Han, and S. Kim, J. Cryst. Growth **254**, 423 (2003).
[23]F. Liu, X. B. Zhang, J. P. Cheng, J. P. Tu, F. Kong, W. Z. Huang, and C. P. Chen, Carbon **41**, 2572 (2003).
[24]N. Pierard, A. Fonseca, Z. Konya, I. Willems, G. Van Tendeloo, and J. B. Nagy, Chem. Phys. Lett. **335**, 1 (2001).
[25]J. Y. Huang, H. Yasuda, and H. Mori, Chem. Phys. Lett. **303**, 130 (1999).